Protease-Activated Receptor 2 Has Pivotal Roles in Cellular Mechanisms Involved in Experimental Periodontitis[▽]

David M. Wong,[1,3,4] Vivian Tam,[1,2] Roselind Lam,[1,2] Katrina A. Walsh,[1,2] Liliana Tatarczuch,[1,3]
Charles N. Pagel,[1,3] Eric C. Reynolds,[1,2] Neil M. O'Brien-Simpson,[1,2]†
Eleanor J. Mackie,[1,3]† and Robert N. Pike[1,4]*†

*CRC for Oral Health Sciences[1] and Melbourne Dental School,[2] University of Melbourne, Carlton, Victoria 3010, Australia;
Faculty of Veterinary Science, University of Melbourne, Parkville, Victoria 3010, Australia[3]; and Department of
Biochemistry and Molecular Biology, Monash University, Victoria 3800, Australia[4]*

The tissue destruction seen in chronic periodontitis is commonly accepted to involve extensive upregulation of the host inflammatory response. Protease-activated receptor 2 (PAR-2)-null mice infected with *Porphyromonas gingivalis* did not display periodontal bone resorption in contrast to wild-type-infected and PAR-1-null-infected mice. Histological examination of tissues confirmed the lowered bone resorption in PAR-2-null mice and identified a substantial decrease in mast cells infiltrating the periodontal tissues of these mice. T cells from *P. gingivalis*-infected or immunized PAR-2-null mice proliferated less in response to antigen than those from wild-type animals. CD90 (Thy1.2) expression on CD4+ and CD8+ T-cell-receptor β (TCRβ) T cells was significantly ($P < 0.001$) decreased in antigen-immunized PAR-2-null mice compared to sham-immunized PAR-2-null mice; this was not observed in wild-type controls. T cells from infected or antigen-immunized PAR-2-null mice had a significantly different Th1/inflammatory cytokine profile from wild-type cells: in particular, gamma interferon, interleukins (interleukin-2, -3, and -17), granulocyte-macrophage colony-stimulating factor, and tumor necrosis factor alpha demonstrated lower expression than wild-type controls. The absence of PAR-2 therefore appears to substantially decrease T-cell activation and the Th1/inflammatory response. Regulation of such proinflammatory mechanisms in T cells and mast cells by PAR-2 suggests a pivotal role in the pathogenesis of the disease.

Protease-activated receptors (PARs) are G-protein-coupled, seven-transmembrane proteins present on many cell types, including epithelial, endothelial, and neuronal cells; T cells; and osteoblasts (1, 37, 39, 48, 57). Rather than being activated solely by ligand occupancy, these receptors are activated by proteolysis of their N terminus to reveal a tethered ligand that interacts with the extracellular loops of the receptor (42).

There are four known PARs; PAR-1, -3, and -4 have thrombin as their usual physiological activator, whereas PAR-2 is activated by a variety of proteases, including trypsin, mast cell tryptase, and neutrophil protease 3 (57). PAR-2 is thought to play pivotal roles in stimulating inflammation, with involvement in increased leukocyte rolling (38), increased epithelial cell permeability (32) and a possible role(s) in chronic arthritis (21).

PAR-2 has been implicated in periodontitis, which is a chronic inflammatory disease associated with the destruction of the periodontal tissues, including bone, leading to tooth loss (23, 28, 47). Chronic periodontitis has also been linked with certain systemic diseases, such as diabetes and cardiovascular diseases. *Porphyromonas gingivalis*, which has been strongly associated with chronic periodontitis (7, 27, 46), produces cysteine proteases known as gingipains (31, 49, 50). The arginine-specific gingipains, RgpA and RgpB, are known to activate PAR-1 and PAR-2, with studies showing that PAR-2 activation by RgpB in oral epithelial cells leads to an increased release of interleukin-6 (IL-6), a known stimulator of osteoclasts, the cells responsible for bone resorption (39). In addition, activation of PAR-2 on gingival epithelial cells by gingipains induces the production of the human β-defensin antimicrobial peptide (14), and RgpB upregulates proinflammatory neuropeptides in dental pulp cells in a PAR-2-dependent manner (56). Other studies have shown that activation of PAR-2 on oral epithelial cells by neutrophil proteases (58) and by human leukocyte elastase and cathepsin G in gingival fibroblasts upregulates IL-8 production (57). IL-8 is a chemokine that activates neutrophils, as well as a chemoattractant that leads neutrophils and T cells to sites of inflammation (5).

The *in vitro* studies mentioned above suggest a proinflammatory role of PAR-2 in periodontitis. Recently, an *in vivo* study showed that oral challenge of rats with a PAR-2 agonist peptide induced many symptoms of periodontitis, such as increased alveolar bone loss and gingival granulocyte infiltration, as well as overexpression of matrix metalloproteinase 2 (MMP-2) and MMP-9 and cyclooxygenase 1 (COX-1) and COX-2 (29). That study suggested that a cascade of events starting with PAR-2 activation induces cytokine release, leading to bone resorption and tissue degradation. Confirmation of the involvement of PAR-2 in experimental periodontitis was provided by a study where PAR-2$^{-/-}$ mice orally challenged with *P. gingivalis* exhibited less alveolar bone loss than did PAR-2$^{+/+}$ challenged mice (28). We have show here that

* Corresponding author. Mailing address: Department of Biochemistry and Molecular Biology, Monash University, Clayton, Victoria 3800, Australia. Phone: 61-3-99029300. Fax: 61-3-99029500. E-mail: rob.pike@med.monash.edu.au.
† N.M.O.-S., E.J.M., and R.N.P. contributed equally to this study.

PAR-2 is involved in a number of the cellular mechanisms that underlie the pathogenesis of experimental periodontitis.

MATERIALS AND METHODS

Animals and materials. Mice in which the PAR-1gene had been disrupted by homologous recombination (16) were kindly provided by S. Coughlin (University of California, San Francisco). These mice have been extensively backcrossed on the C57BL/6J background and were bred at Monash University. Age- and sex-matched C57BL/6J mice were used as wild-type controls. PAR-2-null mice were generated on a 129Sv background by J. Morrison and M. Stevens (52). For experiments utilizing PAR-2$^{-/-}$ mice, PAR-2$^{+/+}$ littermates were used as controls. The mouse colony was maintained by PAR-2$^{+/-}$ × PAR-2$^{+/-}$ matings, and all mice were genotyped by using a PCR-based approach. Experiments making use of animal tissues were approved by the Animal Care and Use Committee of the Department of Biochemistry and Molecular Biology, Monash University (Ethics approval, BAM/B/23/2003). All primers for PCR and quantitative PCR were synthesized by Geneworks (Adelaide, Australia). PCR reagents, such as deoxynucleoside triphosphates, 50-bp DNA ladder, PCR buffer, 25 mM MgCl$_2$, and GoTaq DNA polymerase were purchased from Promega (Madison, WI). *P. gingivalis* strain W50 was grown and harvested as described previously (44, 45) and used as a live inoculum for the mouse periodontitis model. For immunization and T-cell assays *P. gingivalis* cultures were harvested, and the cell pellets were resuspended in 40 ml of 0.5% (vol/vol) formalin overnight at room temperature. Fresh formalin was added the next day, after which the bacteria (formalin-killed W50 [FK-W50]) were ready for use.

Mouse periodontitis model. The mouse periodontitis model was performed as described previously (49) and involved orally inoculating mice with live *P. gingivalis* cells (strain W50). Overall, 24 wild-type and 24 PAR-1 or PAR-2-null mice at 8 weeks of age were used for the experiment. The wild-type and receptor-null mice groups were equally subdivided into groups that were infected with *P. gingivalis* or sham infected. The infection regimen for the periodontitis model was as follows: four doses of 10^{10} bacterial cells 2 days apart, followed by a 10-day break before another four doses of 10^{10} bacterial cells 2 days apart. Mice were killed 4 weeks after the last inoculation, and then the maxillae were removed and dissected into left-half and right-half maxillae for analyses as previously described (49).

Histomorphometric analysis of maxillae. For one-half maxilla from each animal, a digital image of the buccal aspect was captured with an Olympus DP12 digital camera mounted on a dissecting microscope, using OLYSIA BioReport software version 3.2 (Olympus Australia Pty, Ltd., New South Wales, Australia) to assess horizontal bone loss, defined as loss occurring in a horizontal plane, perpendicular to the alveolar bone crest (ABC) that results in a reduction of the crest height. Each half-maxilla was aligned so that the molar buccal and lingual cusps of each image were superimposed, and the image was captured with a micrometer scale in frame, so that measurements could be standardized for each image. The area of exposed root surface, between the cementoenamel junction and the ABC for each molar tooth was measured using the software. These measurements were determined twice by a single blinded examiner using a randomized and coded protocol.

The other half maxillae from three mice of each group were processed for histomorphometry as previously described (2). Briefly, the specimens were fixed, decalcified, and embedded in Spurr's resin. Semithin sections (2 to 5 μm) were stained in 0.5% (wt/vol) methylene blue. Mast cell counts and analysis of alveolar bone resorption (eroded surface) were conducted on images of sections captured with a digital camera (Spot; Diagnostic Instruments, Inc.) linked to an Olympus BX60 microscope. Measurements were made with Image-Pro Plus image analysis software (Media Cybernetics, Silver Spring, MD).

Mast cells were identified as large cells with unilobed nuclei containing numerous intensely metachromatically stained granules in their cytoplasm (Fig. 1b, inset) (4). Mast cells were counted in a specific field located at the base of the gingival sulcus (buccal and lingual aspects) and in between the cementum and alveolar bone (illustrated in Fig. 1a and b). The eroded surface (ES) of the alveolar bone on the buccal aspect was measured in a region extending 450 μm from the ABC toward the apex of the tooth (illustrated in Fig. 1c) and expressed as a percentage of bone surface (BS), that is, ES/BS × 100. For the mast cell counts and the percentage of alveolar surface erosion, results from three sections were averaged to give the result for each animal. The results for mast cell counts and alveolar surface erosion were obtained from three animals per genotype and treatment group. All histomorphometric analyses were performed by a single blinded examiner using a randomized and coded protocol.

Flow cytometric analysis. Mice were immunized (25 μg/mouse with formalin-killed *P. gingivalis* W50 in incomplete Freund adjuvant administered subcutane-

ously to the hind paw), and 7 days later the popliteal and inguinal lymph nodes were removed and the lymph nodes were pooled into their respective groups. Lymphocytes were isolated from the four treatment groups (PAR-2$^{+/+}$ sham immunized, PAR-2$^{+/+}$ immunized, PAR-2$^{-/-}$ sham immunized, and PAR-2$^{-/-}$ immunized) after processing the lymph nodes through a sieve, following which the separated tissue was collected and gently layered onto 5 ml of Lympholyte M and centrifuged (800 × g, 20 min). The lymphocyte layer was collected and washed twice with Dulbecco modified Eagle medium (DMEM) containing 10% (vol/vol) fetal calf serum (FCS), penicillin (100 U/ml), streptomycin sulfate (100 μg/ml) and glutamate. The lymphocytes were counted by using a Coulter particle counter (Beckman Coulter, Fullerton, CA), after which 10^6 cells were added per well for each experimental group on a 96-well plate. The plate was centrifuged at 800 × g for 5 min, and the supernatant was removed. For each treatment group, four wells were used, with two wells for antibody mixture 1 (anti-CD90/Thy-1.2-fluorescein isothiocyanate [FITC], anti-CD8-phycoerythrin [PE] and anti-TCRβ-allophycocyanin [APC]; BD Biosciences, New South Wales, Australia), and two wells for antibody mixture 2 (anti-CD90/Thy-1.2-FITC, anti-CD4-PE, and anti-TCRβ-APC). Both antibody mixtures containing 1% (vol/vol) FC blocker (BD Biosciences) were incubated with shaking for 20 min at room temperature in the dark. Cells alone (PAR-2$^{+/+}$ nonimmunized) and single-color controls (where PAR-2$^{+/+}$ nonimmunized lymphocytes were incubated with one fluorescent antibody) were used as background controls. A Cytomics FC500 flow cytometer (Beckman-Coulter, New South Wales, Australia) was used to detect the stained lymphocytes.

T-cell proliferation and ELISPOT assays. The remaining isolated lymphocytes from the immunized and sham-immunized mice were further purified by using mouse PAN T-cell MAC beads and an Automac bead cell sorter (Miltenyi Biotech, New South Wales, Australia). Spleens were also removed from the sham-immunized mice and pooled into PAR-2$^{+/+}$ and PAR-2$^{-/-}$ groups. Spleens were processed through a sieve, the single-cell suspension was washed twice (800 × g) in DMEM, and the red blood cells were lysed using red cell lysis buffer (Sigma-Aldrich, New South Wales, Australia). After three washes (800 × g) in DMEM, the splenic cells were irradiated (2,200 rads) and used as a source of syngeneic antigen-presenting cells in the T-cell and enzyme-linked immunospot (ELISPOT) assays.

A serial dilution of *P. gingivalis* FK-W50 cells (starting from 25 μg of protein/100 ml) was added to a 96-well tissue culture plate. T cells from the four experimental treatment groups were added in triplicate to the wells containing *P. gingivalis* FK-W50 at a concentration of 10^5 cells/well. PAR-2$^{+/+}$ sham-immunized antigen presenting cells at a concentration of 10^5 cells were added to the wells containing T cells from PAR-2$^{+/+}$ sham-immunized and immunized mice. PAR-2$^{-/-}$ sham-immunized antigen presenting cells were added to the wells containing T cells from PAR-2$^{-/-}$ sham-immunized and immunized mice. For each group, a negative control was used where wells only contained T cells and antigen-presenting cells. Serially diluted concanavalin A was used as a positive control by adding it to wells that contained T cells and antigen-presenting cells.

The plates were incubated at 37°C in 5% CO$_2$ for 3 days, after which 1 μCi of [^{3}H]thymidine (Amersham Biosciences, Buckinghamshire, United Kingdom) was added to the wells, followed by incubation for a further 18 h. After incubation, 40 μl of mammalian cell lysis buffer (Sigma-Aldrich) was added to the wells for 20 min. Cells were subsequently harvested onto glass fiber filter mats using the MACHIII cell harvester (Tomtec, Hamden, CT), and the filter was air dried and sealed into sample bags containing 5 ml of scintillant fluid. A Wallac Microbeta β-scintillation counter instrument (Perkin-Elmer, New South Wales, Australia) was used to count the radioactivity emitted from the glass fiber filter mats, and the counts per minute (cpm) in each well were determined. The mean cpm values for either FK-W50-stimulated or control cells were calculated by averaging the counts in the respective triplicate wells. The stimulatory index (SI) was calculated by dividing the mean cpm obtained after antigen stimulation by the mean cpm detected in control, unstimulated wells.

For the ELISPOT assays, Millipore Multiscreen 96-well filtration plates (MAHAS450; Millipore, New South Wales, Australia) were coated with anti-mouse cytokine capture antibodies (eBiosciences, San Diego, CA), specific for IL-4 and gamma interferon (IFN-γ), at a concentration of 4 μg/ml in 0.1 M sodium bicarbonate buffer (pH 9.5), followed by incubation overnight at 4°C. The ELISPOT plates were washed with Dulbecco phosphate-buffered saline (PBS) and blocked with enriched DMEM for 1 h at 37°C. Lymph node T cells from each group and spleens were prepared as described above. Lymph node cells (10^5/well) from FK-W50-immunized PAR-2$^{+/+}$ or PAR-2$^{-/-}$ mice were incubated with gamma-irradiated (2,200 rads) syngeneic spleen cells as a source of antigen-presenting cells (PAR-2$^{+/+}$ or PAR-2$^{-/-}$, respectively, 10^{5}cells/well) and *P. gingivalis* FK-W50 cells (1.0 μg/ml). Plates were incubated at 37°C in an atmosphere of 5% CO$_2$ in air for 48 h in a humidified incubator, after which they were
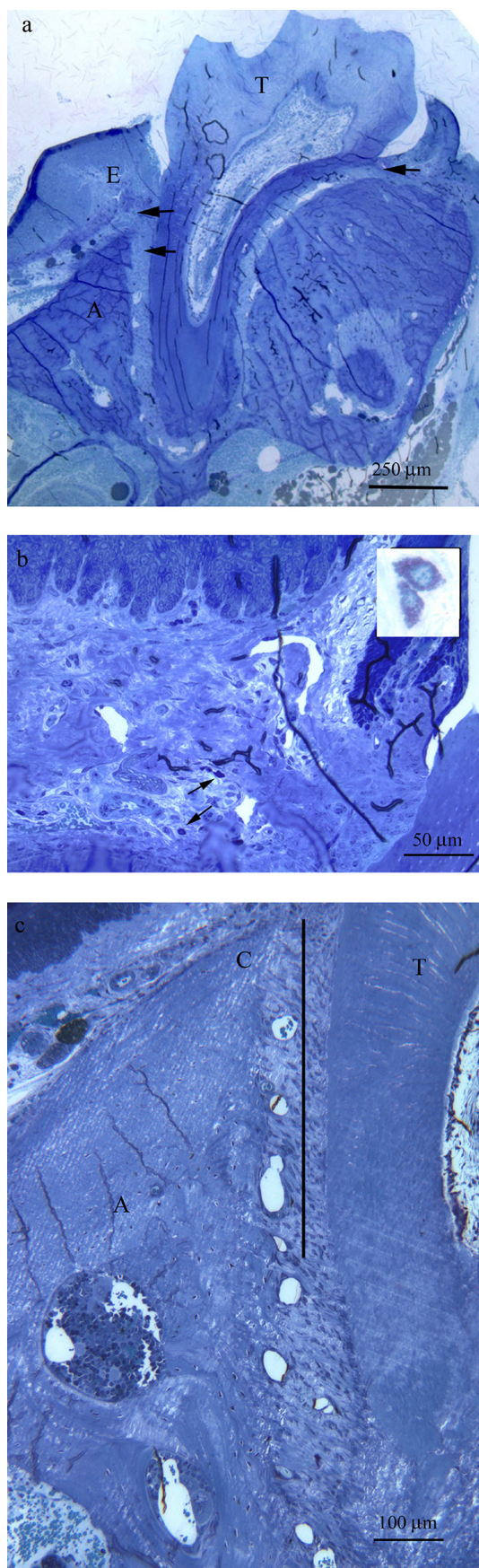
washed with PBS containing 0.05% (vol/vol) Tween 20 (PBST) three times and once with deionized water. Cytokine-specific biotinylated antibodies (eBiosciences, San Diego, CA) specific for IL-4 and IFN-γ were added at a concentration of 2 μg/ml in Dulbecco PBS-enriched DMEM (1:1 [vol/vol]) and incubated at room temperature for 2 h. Plates were washed six times with PBST and streptavidin-alkaline phosphatase conjugate (Roche, Castle Hill, New South Wales, Australia) was added to the plates at a 1:1,000 dilution in Dulbecco PBS-enriched DMEM (1:1 [vol/vol]) and incubated for 1 h at room temperature. The plates were washed with PBST and PBS, after which substrate (5-bromo-4-chloro-3-indolyl phosphate/nitroblue tetrazolium [BCIP/NBT]; Sigma-Aldrich, St. Louis, MO) was added to allow spots to develop for 20 to 30 min, which were counted by using an EliSpot Reader Lite (version 2.9; Autoimmun Diagnostika GmbH, Strassberg, Germany). As described above, ELISPOT studies were also undertaken to analyze the T-cell response in the mouse periodontitis model, where T cells were isolated from the submandibular lymph nodes, which are the gingival tissue draining lymph nodes. Statistical analysis of the ELISPOT data was carried out on the data represented as spot-forming cells (SFC)/million, SFC/million minus control, and also as a ratio (test/control variable), where appropriate. All analyses gave the same results, but only data for SFC/million and SFC/million minus control are shown.

Bio-Plex cytokine array. For the simultaneous quantitation of multiple secreted cytokines, undiluted supernatants were collected from three separate T-cell proliferation assays where T cells obtained from FK-W50-immunized PAR-2$^{+/+}$ and PAR-2$^{-/-}$ mice were exposed to 0.78 μg of *P. gingivalis* FK-W50/ml (see Fig. 6) and were analyzed by using a mouse cytokine kit containing IL-2, IL-3, IL-4, IL-5, IL-6, IL-9, IL-10, IL-12 (p70), IL-13, IL-17, granulocyte-macrophage colony-stimulating factor (GM-CSF), IFN-γ, and tumor necrosis factor alpha (TNF-α) beads on the Bio-Plex suspension array system (Bio-Rad, Hercules, CA) according to the manufacturer's instructions. Standard curves were prepared, and samples were analyzed by using the Bio-Plex Manager software on the Bio-Plex 2200 instrument. The concentrations of these cytokines in the supernatants from each T-cell assay were analyzed in triplicate, and the results were averaged.

Statistical analysis. Bone loss (mm^2) data were statistically analyzed by using a one-way analysis of variance, Dunnett's 3T test, and Cohen's effect size (d). Cohen's effect sizes (15) were calculated using an effect size calculator provided online (http://cem.dur.ac.uk/ebeuk/researc/effectsize/). According to Cohen (15), a small effect size (d) is ≥0.2 and <0.5, a moderate effect size is ≥0.5 and <0.8, and a large effect size is ≥0.8. All other data were statistically analyzed by using the Student t test and Cohen's effect size, and the results are expressed as the means ± the standard errors of the mean (SEM). The significance of differences between experimental groups was determined with the Student t test, assuming unequal variances. P values of <0.05 were considered significant.

RESULTS

Role(s) of PAR-1 and PAR-2 in *P. gingivalis*-induced alveolar bone resorption. To determine whether PAR-1 or PAR-2 have a role in *P. gingivalis*-induced periodontal bone loss, PAR-1$^{+/+}$ and PAR-1$^{-/-}$ mice and PAR-2$^{-/-}$ and PAR-2$^{+/+}$ littermates were orally infected with *P. gingivalis* strain W50, and the alveolar bone loss induced was analyzed. The maxillae of PAR-1$^{+/+}$, PAR-1$^{-/-}$, and PAR-2$^{+/+}$ mice orally infected with *P. gingivalis* W50 had a significantly ($P < 0.05$) greater area of exposed root surface than the sham-infected groups, indicating that the infection had resulted in alveolar bone loss (Fig. 2). There was no significant difference between PAR-

FIG. 1. Regions used for histomorphometry in sections of mouse maxillae. (a) Section of a maxilla from a PAR-2$^{+/+}$ mouse after challenge with *P. gingivalis*. The arrows indicate the fields in which the mast cells were counted. E, gingival epithelium; T, tooth; A, alveolar bone. (b) Section showing two mast cells (arrows); insert shows mast cells at higher magnification. (c) Section of a maxilla showing the field taken for measuring the eroded surface of the alveolar bone. The bold line indicates the region of interest, which is 450 μm in length. C, alveolar bone crest; T, tooth.
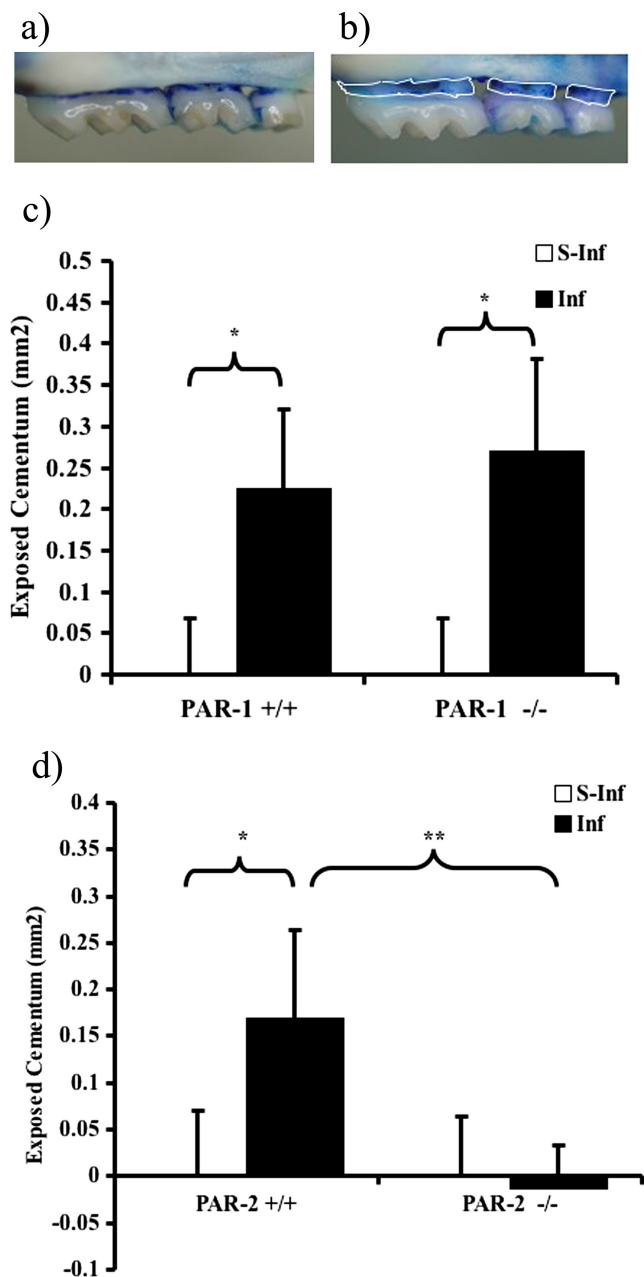
FIG. 2. Quantification of periodontal bone loss, in PAR-1 (+/+ and −/−) and PAR-2 (+/+ and −/−) mice in experimental periodontitis. Half maxillae from PAR-2^{−/−} (a) and PAR-2^{+/+} (b) mice orally infected with *P. gingivalis* W50 were stained with methylene blue. The area of exposed root surface (outlined by white lines in panel b) was measured and counted blind by one evaluator. The results for the comparison between infected and sham-infected PAR-1^{+/+} and PAR-1^{−/−} (c) and PAR-2^{+/+} and PAR-2^{−/−} (d) mice are shown as means ± SEM (*n* = 12; *, *P* < 0.05; **, *P* < 0.01) .

1[+/+] and PAR-1^{−/−} infected mice in terms of the exposed root surface (Fig. 2c). However, the PAR-2^{−/−} mice orally infected with *P. gingivalis* W50 were found to have significantly (*P* < 0.01) less exposed root surface than their respective PAR-2^{+/+} counterparts (Fig. 2d). Moreover, there was no significant difference in the values between the PAR-2^{−/−} mice that were
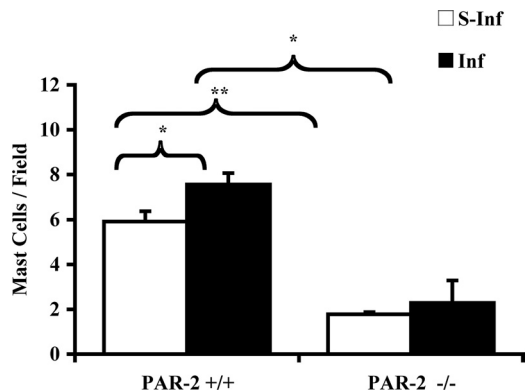

FIG. 3. Quantification of the number of mast cells in the periodontal tissue of mice orally challenged with *P. gingivalis* W50. The results are presented as the mean ± the SEM (*n* = 3). *, *P* < 0.05; **, *P* < 0.01 (for comparisons indicated by lines above the bars). S-Inf, sham-infected mice; Inf, infected mice.

orally infected with *P. gingivalis* and the sham-infected PAR-2^{−/−} or PAR-2^{+/+} mice.

Histological examination of mast cells in periodontal tissue. In the histological analysis (Fig. 1), mast cells were found in higher numbers in the periodontal tissue of PAR-2^{+/+} mice orally infected with *P. gingivalis* compared to sham-infected PAR-2^{+/+} mice. In contrast, *P. gingivalis* oral infection had no effect on mast cell numbers in PAR-2^{−/−} mice. It is noteworthy that sham-infected PAR-2^{−/−} mice were also found to have significantly fewer mast cells in their periodontal tissue than PAR-2^{+/+} unchallenged mice (Fig. 3).

Eroded surface, as a histomorphometric parameter of recent bone resorption, was greater in alveolar bone from PAR-2^{+/+} mice orally infected with *P. gingivalis* than in alveolar bone from their sham-infected counterparts (Fig. 4). There was no difference in the alveolar bone eroded surface between *P. gingivalis*-infected and sham-infected PAR-2^{−/−} mice.
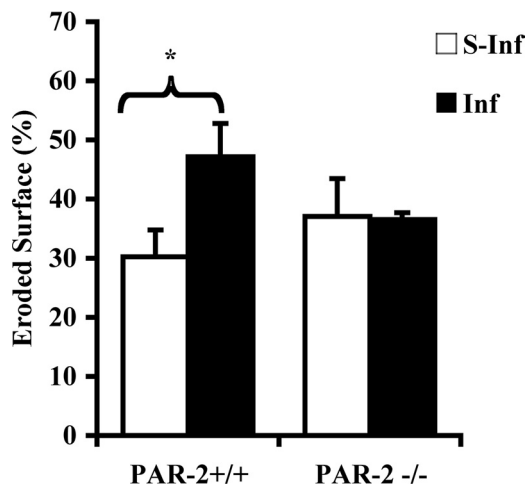

FIG. 4. Eroded bone surface measurements in sections of mouse maxillae (see Fig. 1c). The results are presented as means ± the SEM (*n* = 3; *, *P* < 0.05 for comparison between infected and sham-infected mice). S-Inf, sham-infected mice; Inf, infected mice.
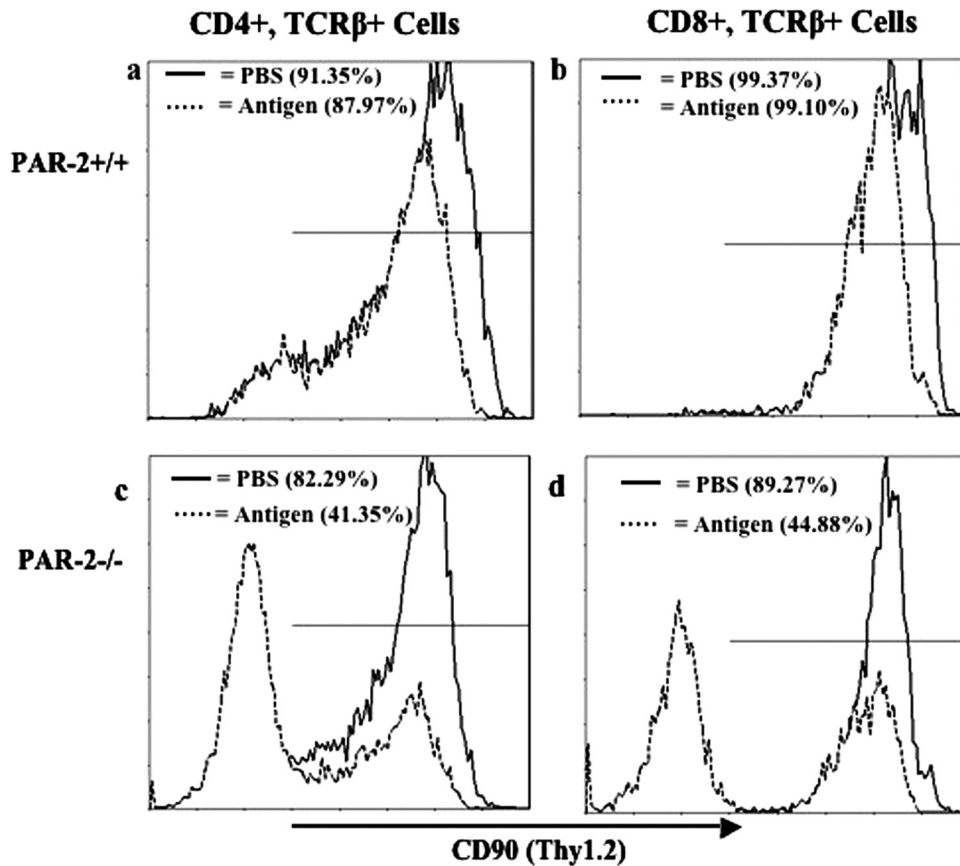
FIG. 5. Expression of CD90 on T cells of PAR-2$^{+/+}$ and PAR-2$^{-/-}$ mice immunized with *P. gingivalis* FK-W50. Lymphocytes were isolated from inguinal and popliteal lymph nodes of mice 7 days after immunization. Expression of molecules on T-cell subsets was detected by FACS analysis with relevant antibodies. The data, expressed as cytometry histograms, are representative of three independent experiments. CD90 expression of T-cell (TCRβ$^+$) subsets (CD4$^+$ and CD8$^+$) is represented by a solid line for PBS-immunized mice (control) and a dashed line for antigen (*P. gingivalis* FK-W50)-immunized mice for the PAR-2$^{+/+}$ isolated lymphocytes (a and b) and for the PAR-2$^{-/-}$ isolated lymphocytes (c and d). A total of 10,000 events were measured.

PAR-2$^{-/-}$ mice display impaired T-cell immune responses. Initially, T cells from mice that had been immunized with *P. gingivalis* FK-W50 cells were isolated by using CD90 (Thy1.2) microbeads to positively select for T cells. However, we consistently obtained poor yields (~10^5 total cells) of T cells from the PAR-2$^{-/-}$ immunized mice, whereas for the PAR-2$^{+/+}$ immunized mice we obtained a typical yield ranging from 3 × 10^7 to 7 × 10^7 T cells. Preliminary phenotyping of the lymphocyte populations from the PAR-2$^{+/+}$ and PAR-2$^{-/-}$ mice indicated that there was no significant difference in the numbers of TCRβ$^+$, CD4$^+$, or CD8$^+$ T cells between the strains of mice (data not shown).

Thus, T cells were isolated from both strains of mice by negative sorting using PAN T-cell microbeads (depleting all lymphocytes except T cells), and we obtained cell numbers in the typical (higher) yield range above for both genotypes using this strategy. Phenotyping analysis of the lymphocyte populations from *P. gingivalis* FK-W50-immunized and sham-immunized (PBS) PAR-2$^{+/+}$ and PAR-2$^{-/-}$ mice by flow cytometry indicated differing expression levels of CD90/Thy-1.2 (Fig. 5). In the PAR-2$^{+/+}$ mice there was no significant difference between the nonimmunized and immunized animals in CD90/Thy-1.2 expression in TCRβ$^+$ CD4$^+$ T cells or TCRβ$^+$ CD8$^+$

T cells (Fig. 5a and b). However, there was a significant ($P <$ 0.001) decrease in CD90/Thy-1.2 expression in both TCRβ$^+$ CD4$^+$ T cells and TCRβ$^+$ CD8$^+$ T cells from immunized compared to sham-immunized PAR-2$^{-/-}$ mice (Fig. 5c and d). Furthermore, in PAR-2$^{-/-}$ immunized mice, 59% of TCRβ$^+$ CD4$^+$ T-cell populations and 55% of TCRβ$^+$ CD8$^+$ T-cell populations were determined to have no CD90/Thy-1.2 expression (data not shown). In comparing the CD90/Thy-1.2 expression in sham-immunized mice, the PAR-2$^{-/-}$ mice had significantly ($P <$ 0.01) less CD90/Thy-1.2$^+$ in CD4$^+$ and CD8$^+$ T cells than their PAR-2$^{+/+}$ counterparts. Interestingly, in the PAR-2$^{+/+}$ mice, although there was no significant difference in the CD4$^+$ or CD8$^+$ T-cell populations positive for CD90/Thy-1.2, there was an observed decrease in CD90/Thy-1.2 expression (as determined by the mean fluorescence intensity) in both T-cell populations in the immunized groups compared to the sham-immunized groups.

To further examine differences in the T-cell populations, cells isolated (using PAN-T microbeads) from PAR-2$^{+/+}$ and PAR-2$^{-/-}$ mice immunized with *P. gingivalis* FK-W50 were subjected to proliferation and cytokine analysis in response to *P. gingivalis* W50 cells. Figure 6 shows that the *P. gingivalis* FK-W50-primed T cells from PAR-2$^{-/-}$ mice had significantly
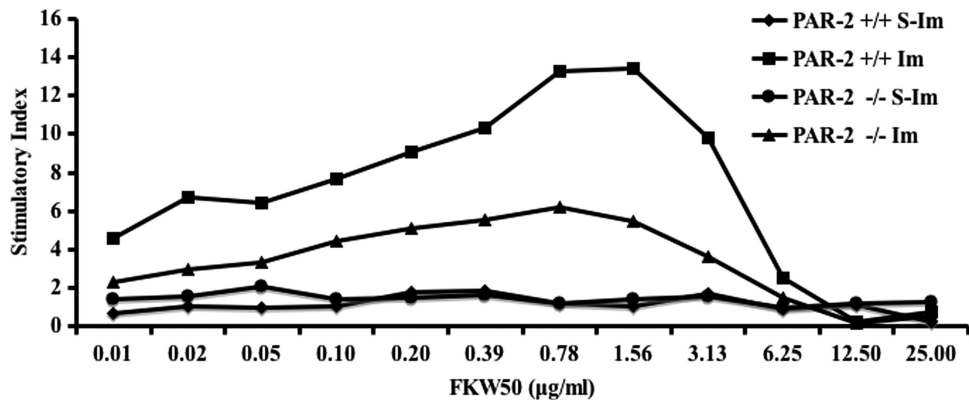
FIG. 6. T-cell proliferation assay. T cells isolated from the lymph nodes of mice 7 days after immunization were incubated with serially diluted *P. gingivalis* FK-W50 antigen in the presence of gamma-irradiated syngeneic antigen presenting cells *in vitro*. The T-cell proliferation was measured by determining the [³H]thymidine incorporation, with the results presented as the stimulatory index (SI), calculated by dividing the mean cpm obtained after antigen stimulation by the mean cpm detected in control, unstimulated wells. This graph is a representation of four independent experiments with similar results. S-Im, sham-immunized mice; Im, immunized mice.

($P < 0.05$) lower maximal proliferation in response to *P. gingivalis* than their PAR-$2^{+/+}$ counterparts. Furthermore, the numbers of IL-4- and IFN-γ-secreting T cells from *P. gingivalis* FK-W50-immunized PAR-$2^{-/-}$ mice were significantly ($P <$ 0.05) less than their PAR-$2^{+/+}$ counterparts (Fig. 7a), with a large difference in the IFN-γ response ($d = 7.49$, 95% confidence interval [CI] = 12.88 to 3.22) compared to the IL-4 response ($d = 5.25$, 95% CI = 7.42 to 1.46). On comparing the
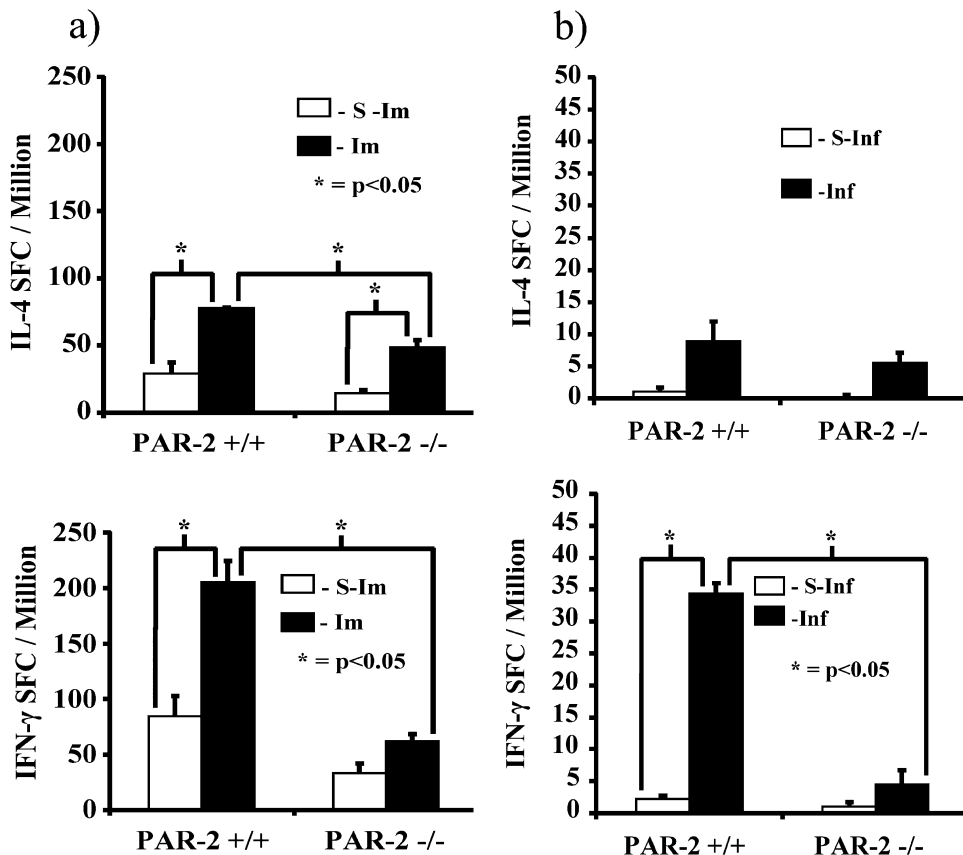

FIG. 7. Cytokine responses of *P. gingivalis* FK-W50-primed T cells from PAR-$2^{+/+}$ and PAR-$2^{-/-}$ mice. T cells isolated from inguinal and popliteal lymph nodes of mice 7 days after immunization (a) and T cells isolated from submandibular lymph nodes (b) from the mouse periodontitis model were stimulated with *P. gingivalis* FK-W50 (1 μg/ml) in the presence of gamma-irradiated syngeneic antigen-presenting cells *in vitro*. After 2 days, the assay was stopped and developed. The data are expressed as SFC/million ± the SD minus the background and are the averages of triplicate assays. S-Im, sham-immunized mice; Im, immunized mice; S-Inf, sham-infected mice; Inf, infected mice.

IL-4 and IFN-γ response in each strain, the PAR-2$^{+/+}$ mice had a significantly ($P < 0.05$) higher IFN-γ response compared to the IL-4 response. In contrast, the number of IFN-γ-secreting T cells was not significantly higher than the number of IL-4-secreting T cells in PAR-2$^{-/-}$ mice; in fact, the mean number of IL-4-secreting T cells was slightly higher ($d = 0.91$, 95% CI = -0.86 to 2.46).

In the mouse experimental periodontitis model, T cells were also isolated and used in an ELISPOT assay to determine the numbers of IL-4- and IFN-γ-secreting T cells in response to *P. gingivalis* stimulation. No significant difference was found in the numbers of IL-4-secreting T cells between PAR-2$^{+/+}$ and PAR-2$^{-/-}$ mice orally infected with *P. gingivalis* (Fig. 7b). However, there was a significantly higher number of IFN-γ-secreting PAR-2$^{+/+}$ T cells compared to PAR-2$^{-/-}$ T cells ($P < 0.05$, $d = 19.58$). Furthermore, in PAR-2$^{+/+}$ mice orally infected with *P. gingivalis* there were significantly higher numbers of IFN-γ-secreting T cells than IL-4-secreting T cells ($P < 0.05$, days = 8.34). However, in the PAR-2$^{-/-}$ mice orally infected with *P. gingivalis*, there was no significant difference between the numbers of IL-4-secreting T cells and IFN-γ-secreting T cells; in fact, the mean number of IL-4-secreting T cells was slightly higher ($d = 0.97$, 95% CI = -0.77 to 2.59).

To further characterize the T-cell cytokine response, the supernatants from the T-cell proliferation assays were analyzed by Bioplex cytokine array for the presence of the following cytokines: IL-2, IL-3, IL-4, IL-5, IL-6, IL-9, IL-10, IL-12 (p70), IL-13, IL-17, GM-CSF, IFN-γ, and TNF-α. T cells from *P. gingivalis*-immunized PAR-2$^{+/+}$ mice secreted significantly ($P < 0.05$) higher amounts of IL-2, IL-3, IL-12 (p70), IL-17, GM-CSF, IFN-γ, and TNF-α than their PAR-2$^{-/-}$ counterparts in response to *P. gingivalis* FK-W50 (Fig. 8). The strongest response (fourfold higher than other cytokines) in both PAR-2$^{+/+}$ and PAR-2$^{-/-}$ T cells, was the level of IL-17 (145.8 ± 69.4 pg/ml and 14.4 ± 4.9 pg/ml for PAR-2$^{+/+}$ and PAR-2$^{-/-}$, respectively). Although there was no significant difference in the levels of the other cytokines analyzed, there were higher numbers (as determined by effect size) of PAR-2$^{+/+}$ T cells secreting IL-5, IL-6, IL-9, IL-10, and IL-13, but not IL-4, than PAR-2$^{-/-}$ T cells ($d = 0.87$, 1.24, 0.67, 0.89, and 0.97, respectively). Furthermore, although analysis of the levels of secreted cytokines showed that no significant difference was observed (Student t test), PAR-2$^{+/+}$ T cells did secrete higher concentrations of IL-5, IL-6, IL-9, IL-10, and IL-13 than were secreted by PAR-2$^{-/-}$ T cells ($d = 0.87$, 1.24, 0.67, 0.89, and 0.97, respectively, as analyzed by Cohen's effect size). Overall, Fig. 6, 7, and 8 show that the proliferation and cytokine secretion responses to antigen of T cells from PAR-2$^{-/-}$ animals were significantly lower compared to T cells from PAR-2$^{+/+}$ animals.

DISCUSSION

PAR-2 can be activated by several proteases, including trypsin, mast cell tryptase and the gingipains from *P. gingivalis* (28, 48). Here we have shown that PAR-2 apparently plays a pivotal role in the progression of the inflammatory events that underpin the pathogenesis of experimental periodontitis. Chronic periodontitis is commonly viewed as an inflammatory condition involving a host response to bacterial components that
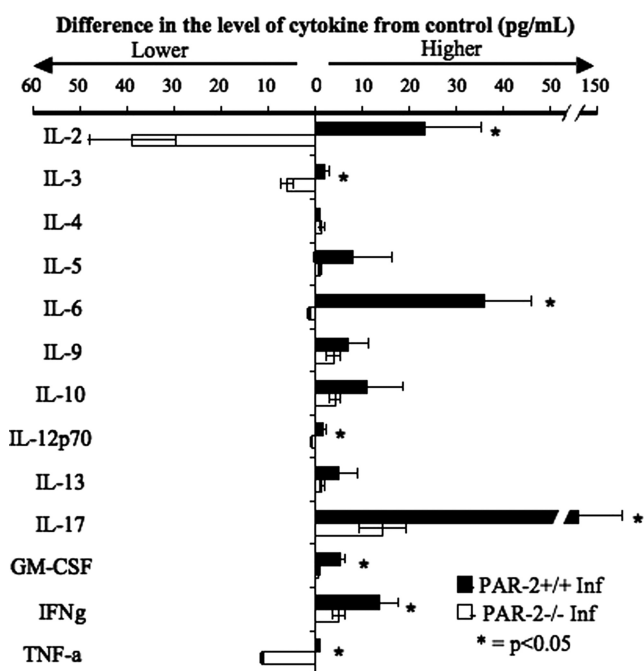

FIG. 8. Cytokine secretion responses of T cells from PAR-2$^{+/+}$ and PAR-2$^{-/-}$ mice to stimulation with *P. gingivalis* FK-W50 antigen. T cells isolated from inguinal and popliteal lymph nodes of mice (PAR-2$^{+/+}$ and PAR-2$^{-/-}$) 7 days after immunization in the hind limb were stimulated with *P. gingivalis* FK-W50 in the presence of gamma-irradiated syngeneic antigen-presenting cells *in vitro*. Supernatants from the T-cell proliferation assays (Fig. 6) were collected, and supernatants corresponding to maximal T-cell proliferation in response to *P. gingivalis* FK-W50 antigen (0.78 μg/ml, Fig. 6) were analyzed for IL-2, IL-3, IL-4, IL-5, IL-6, IL-9, IL-10, IL-12p70, IL-13, IL-17, GM-CSF, IFN-γ, and TNF-α by using the Bio-Plex cytokine array system. The data are expressed in pg/ml minus the no-antigen control and are representative of three independent T-cell proliferation assays. Sample size, $n = 3$.

have diffused into the subjacent gingival tissue from the subgingival plaque biofilm. The inability of the host immune system to remove the biofilm, which is external to the tissue and accreted on a nonshedding tooth root surface, results in continual external stimulation, leading to a chronic inflammatory state. This chronic inflammation leads to periodontal tissue damage, including bone resorption caused by the cells and molecules of the host system response (23, 46, 47).

P. gingivalis, a major causative agent of chronic periodontitis, was orally inoculated into PAR-1$^{+/+}$, PAR-1$^{-/-}$, PAR-2$^{+/+}$, and PAR-2$^{-/-}$ mice to induce disease. Essentially, no difference was found between PAR-1$^{+/+}$ and PAR-1$^{-/-}$ mice in the model, indicating that this receptor does not play a pivotal role in the progression of experimental periodontitis. However, it was clearly shown that less alveolar bone resorption occurred in mice lacking the PAR-2 gene, confirming the bone loss findings of Holzhausen et al. (28). In the present study, further histological, cellular, and molecular analysis was carried out to investigate the immunological mechanisms involved in the reduction of bone loss in the PAR-2-null mice in response to oral infection with *P. gingivalis*.

Histological analyses indicated that the increased numbers of mast cells seen in the maxillary tissue of infected PAR-2$^{+/+}$ mice were not seen in infected PAR-2$^{-/-}$ mice. It must be

noted that in sham-infected animals, there were also significantly fewer mast cells in the tissue of PAR-2$^{-/-}$ mice compared to the PAR-2$^{+/+}$ mice, indicating that the lack of PAR-2 may also have a role in mast cell differentiation or infiltration into tissues. Thus, activation of PAR-2 expressed by mast cells (19, 55) may participate in the recruitment of these cells. Mast cells can be activated by bacterial antigens (33, 35, 53), leading to the release of inflammatory mediators that are pivotal to the innate immune response (20, 22, 54). These cells may therefore play a pivotal role in the early inflammatory response to *P. gingivalis* in chronic periodontitis. This may result from activation of PAR-2 on their surface by the arginine-specific gingipains or other tissue proteases, as well as other mechanisms of activation. It has been shown that activation of PAR-2 on mast cells leads to degranulation by these cells, causing the release of proinflammatory compounds that kill pathogens and upregulate the immune response (3). Mast cell tryptase, released from the granules of these cells upon activation, activates PAR-2 (17), and therefore these cells could play a primary role in periodontitis by causing the activation of the receptor on other cells in the periodontal tissues.

These results indicate that PAR-2 may have a role in the innate immune response to *P. gingivalis*, so the next question was whether PAR-2 was involved in the adaptive immune response. T cells obtained from the lymph nodes of PAR-2$^{-/-}$ mice that were immunized with formalin-killed *P. gingivalis* W50 proliferated significantly less in response to antigen than T cells from PAR-2$^{+/+}$ immunized mice. This is consistent with previous observations (43), noting a marked difference in proliferation between T cells from PAR-2$^{+/+}$ and PAR-2$^{-/-}$ myelin oligodendrocyte glycoprotein-immunized mice. The decreased proliferation of T cells is another plausible reason for the reduction in bone loss seen in the PAR-2$^{-/-}$ mice in the mouse periodontitis model, since impairment in T-cell activation would lead to a less effective immune response, thereby also decreasing the tissue damage associated with the inflammatory response. Studies have also shown that major histocompatibility complex class II-null and CD4-null mice have less periodontal bone loss when challenged with *P. gingivalis* compared to wild-type mice (6, 8, 9).

It was noted in both the periodontitis model and the immunization experiments that use of the pan-T-cell marker, CD90/Thy-1, for isolation of T cells led to poor recovery of cells from PAR-2$^{-/-}$ mice, indicating a decreased expression of CD90/Thy-1 compared to wild-type controls. fluorescence-activated cell sorting (FACS) analysis of whole lymph node lymphocyte isolates verified this hypothesis since expression of CD90/Thy-1 was markedly downregulated after immunization in PAR-2$^{-/-}$ mice, with the majority of CD4$^+$ and CD8$^+$ T cells being CD90/Thy-1 negative. CD90/Thy-1 has important roles in T-cell activation and maturation (25), possibly due to its action as coreceptor for the T-cell receptor, which may act as a *cis* ligand for Thy-1 (10, 24). Thy-1 also regulates cell adhesion and migration (51), thus lower levels of this receptor would have a detrimental effect on T-cell migration to sites of infection and thereby decrease their contribution to inflammation. Thus, the marked downregulation of expression of CD90/Thy-1 in T cells from immunized PAR-2$^{-/-}$ mice might contribute to the reduced proliferation of the T cells from PAR-2$^{-/-}$ mice noted here and previously (43). It is also possible

that the reduction of expression of Thy-1 might influence the profile of cytokines expressed by T cells from the PAR-2$^{-/-}$ mice.

ELISPOT analysis of T cells from both immunized and infected wild-type mice showed strongly increased IFN-γ-positive T-cell colonies compared to IL-4-positive colonies upon stimulation by the bacterium. The pronounced increase in IFN-γ-positive colonies upon immunization or infection was not seen for the T cells from PAR-2$^{-/-}$ mice. The increase in IFN-γ-secreting T cells from wild-type mice would be expected to induce a strong T-cell helper 1 (Th1) type of immune response, which would likely contribute strongly to the tissue destruction observed in periodontitis. In the PAR-2$^{-/-}$ mice, most T cells were Thy-1 negative after antigen stimulation, which may affect the T-cell activation state and thus the production of cytokines. Interestingly, naturally occurring Thy-1 negative CD4$^+$ T-cell populations only secrete IL-4 and not IFN-γ (13). Our data suggest that the antigen-induced downregulation of Thy-1 resulting in CD4$^+$ and CD8$^+$ Thy-1 negative T cells results in a "deactivated" T-cell population. The findings from the present study therefore suggest that antigen stimulation of PAR-2$^{-/-}$ T cells results in a downregulation of CD90/Thy-1, leading to deactivated cells that are unable to contribute to an inflammatory response and thus induction of tissue destruction. This is consistent with our results showing a pronounced decrease in bone resorption in the receptor-null mice. These findings also point to the potential use of a PAR-2 antagonist to restrict the contribution of T cells to inflammation, as has been shown in mouse models of rheumatoid arthritis (34), a disease known to be modulated by T cells.

Supernatants from the T-cell proliferation experiments were tested for the levels of a range of cytokines to further understand the role of PAR-2 in these cells. The levels of IL-2, which plays a vital role in T-cell proliferative responses, were markedly downregulated in the supernatants of T cells from PAR-2$^{-/-}$ mice, which provides an explanation for the lack of proliferation by T cells from these mice. The levels of other cytokines were also affected, including the reduction of IFN-γ expression, a finding consistent with the results of the ELISPOT assays. IL-17 protein levels were highly upregulated in the supernatants of T cells from PAR-2$^{+/+}$ mice and were ~10-fold higher than in supernatants of T cells from PAR-2$^{-/-}$ immunized mice. Notably, there was no difference between the supernatants from PAR-2$^{+/+}$ versus PAR-2$^{-/-}$ derived T cells in the sham-immunized mice, suggesting that the differences reflected events occurring during an immune response to antigen. The cells responsible for the expression of IL-17 have been identified as a subset of T cells (Th$_{17}$) (26). IL-17 is a potent inducer of inflammation and studies have shown it to be involved in autoimmune diseases such as rheumatoid arthritis (40, 41). Recent studies have reported that the IL-17 levels in gingival samples are higher in periodontitis patients than healthy patients, indicating that Th17 cells may play a significant role in the inflammatory response associated with chronic periodontitis (12, 30, 59). Since PAR-2 activation in a variety of cells causes upregulation of IL-6, a potent inducer of Th$_{17}$ cell production (11), this pathway could be involved in the upregulation of IL-17 levels seen in the T-cell supernatants from PAR-2$^{+/+}$ mice and thus the lower levels of

IL-17 seen in the PAR2$^{-/-}$ mice may be a consequence of the lower levels of IL-6 observed.

In addition to the highly altered cytokine levels noted above, it is worth noting that almost every cytokine tested showed a difference between the PAR-2$^{-/-}$ and the PAR-2$^{+/+}$ derived cells, with the levels of IL-3, IL-12p70, GM-CSF, and TNF-α all significantly decreased in the samples from PAR-2$^{-/-}$ mice. These data suggest that although the CD4 and CD8 T-cell population numbers in PAR-2$^{-/-}$ mice are similar to those in PAR-2$^{+/+}$ mice, upon antigen activation, potential inflammatory T cells become less active, resulting in reduced proliferation, cytokine secretion, and downregulation of CD90/Thy-1. The reduction in the inflammatory T-cell response in PAR-2$^{-/-}$ mice fits with the receptor's role in stimulating inflammation. Proliferation of T cells from the PAR-2$^{-/-}$ mice was not completely prevented; this may be due to a response by CD90/Thy-1-negative T cells, a small population of cells that secrete IL-4 in response to antigen, but not IFN-γ (13). We found a low level of proliferation of T cells in PAR-2$^{-/-}$ mice despite there being similar or higher numbers of IL-4-secreting T cells in the population compared to PAR-2$^{+/+}$ mice. This indicates that Th2 and/or CD90/Thy-1-negative cells may be stimulated by antigen in the PAR-2$^{-/-}$ mice, resulting in proliferation and IL-4 secretion that is not regulated by the inflammatory/Th1 T cells that would normally be the major responsive population to bacterial infection. Notably, the absence of Thy-1 from T cells has been shown to profoundly affect T-cell signaling through the T-cell receptor and CD3 (36); thus, the downregulation of this receptor on PAR-2-negative T cells may have caused a widespread effect on the ability of these cells to be activated by antigen. The molecular basis for the effect of PAR-2 on Thy-1 levels will be an interesting avenue for future research.

The role of PAR-2 in periodontal disease progression needs to be considered at several levels. First, *P. gingivalis* releases arginine-specific gingipains, which may penetrate gingival tissue and activate PAR-2 on epithelial, endothelial, and connective tissue cells, thus causing an inflammatory response. One of the possible outcomes of such activation of PAR-2 is the production of IL-6 by gingival epithelial cells. IL-6 is a proinflammatory cytokine that can directly promote the resorption of bone through the induction of osteoclast formation, and it is possible that this pathway operates to cause bone loss in periodontal disease (39). Second, mast cells attracted to the site of inflammation could also recognize *P. gingivalis*, causing them to release TNF-α, which would recruit neutrophils to the site of infection, and mast cell tryptase, which would activate PAR-2 on surrounding cells. Third, the recruitment of neutrophils would add more potential activators of PAR-2 as neutrophils produce proteinase-3, which is another known activator of PAR-2 (18). The activation of PAR-2 by the gingipains, tryptase, and proteinase 3 may all lead to activation and proliferation of T cells, strongly upregulating a tissue destructive immune response. Due to the multiple potential levels of activation of the receptor during the inflammatory process, it is therefore highly possible that in its absence, the inflammatory response to the bacterium is markedly reduced, thereby decreasing host tissue degradation and bone resorption. Our findings strongly indicate the potential for antagonists of PAR-2 as a treatment for periodontitis and potentially other chronic inflammatory diseases.

REFERENCES

1. **Abraham, L. A., C. Chinni, A. L. Jenkins, A. Lourbakos, N. Ally, R. N. Pike, and E. J. Mackie.** 2000. Expression of protease-activated receptor-2 by osteoblasts. Bone **26:**7–14.
2. **Ahmed, Y. A., L. Tatarczuch, C. N. Pagel, H. M. Davies, M. Mirams, and E. J. Mackie.** 2007. Physiological death of hypertrophic chondrocytes. Osteoarthritis Cartilage **15:**575–586.
3. **Alshurafa, H. N., G. R. Stenton, J. L. Wallace, M. D. Hollenberg, A. D. Befus, and H. Vliagoftis.** 2004. A protease activated receptor-2 (PAR-2) activating peptide, tc-LIGRLO-NH2, induces protease release from mast cells: role in TNF degradation. BMC Pharmacol. **4:**12–20.
4. **Bacha, W., et al.** 2000. Color atlas of veterinary histology, 2nd ed. Lippincott/The Williams & Wilkins Co., Baltimore, MD.
5. **Baggiolini, M., B. Dewald, and B. Moser.** 1994. Interleukin-8 and related chemotactic cytokines—CXC and CC chemokines. Adv. Immunol. **55:**97–179.
6. **Baker, P. J., M. Dixon, R. T. Evans, L. Dufour, E. Johnson, and D. C. Roopenian.** 1999. CD4$^+$ T cells and the proinflammatory cytokines gamma interferon and interleukin-6 contribute to alveolar bone loss in mice. Infect. Immun. **67:**2804–2809.
7. **Baker, P. J., R. T. Evans, and D. C. Roopenian.** 1994. Oral infection with *Porphyromonas gingivalis* and induced alveolar bone loss in immunocompetent and severe combined immunodeficient mice. Arch. Oral Biol. **39:**1035–1040.
8. **Baker, P. J., J. Garneau, L. Howe, and D. C. Roopenian.** 2001. T-cell contributions to alveolar bone loss in response to oral infection with *Porphyromonas gingivalis*. Acta Odontol. Scand. **59:**222–225.
9. **Baker, P. J., L. Howe, J. Garneau, and D. C. Roopenian.** 2002. T-cell knockout mice have diminished alveolar bone loss after oral infection with *Porphyromonas gingivalis*. FEMS Immunol. Med. Microbiol. **34:**45–50.
10. **Barker, T. H., and J. S. Hagood.** 2008. Getting a grip on Thy-1 signaling. Biochim. Biophys. Acta **1793:**921–923.
11. **Bettelli, E., Y. Carrier, W. Gao, T. Korn, T. B. Strom, M. Oukka, H. L. Weiner, and V. K. Kuchroo.** 2006. Reciprocal developmental pathways for the generation of pathogenic effector TH17 and regulatory T cells. Nature **441:**235–238.
12. **Cardoso, C. R., G. P. Garlet, G. E. Crippa, A. L. Rosa, W. M. Junior, M. A. Rossi, and J. S. Silva.** 2009. Evidence of the presence of T helper type 17 cells in chronic lesions of human periodontal disease. Oral Microbiol. Immunol. **24:**1–6.
13. **Cerasoli, D. M., G. Kelsoe, and M. Sarzotti.** 2001. CD4$^+$ Thy1$^-$ thymocytes with a Th-type 2 cytokine response. Int. Immunol. **13:**75–83.
14. **Chung, W. O., S. R. Hansen, D. Rao, and B. A. Dale.** 2004. Protease-activated receptor signaling increases epithelial antimicrobial peptide expression. J. Immunol. **173:**5165–5170.
15. **Cohen, J.** 1969. Statistical power analysis for the behavioral sciences. Lawrence Erlbaum Associates, Hillsdale, CA.
16. **Connolly, A. J., H. Ishihara, M. L. Kahn, R. V. Farese, Jr., and S. R. Coughlin.** 1996. Role of the thrombin receptor in development and evidence for a second receptor. Nature **381:**516–519.
17. **Corvera, C. U., O. Dery, K. McConalogue, S. K. Bohm, L. M. Khitin, G. H. Caughey, D. G. Payan, and N. W. Bunnett.** 1997. Mast cell tryptase regulates rat colonic myocytes through proteinase-activated receptor 2. J. Clin. Invest. **100:**1383–1393.
18. **Coughlin, S. R., and E. Camerer.** 2003. Participation in inflammation. J. Clin. Invest. **111:**25–27.
19. **D'Andrea, M. R., C. J. Rogahn, and P. Andrade-Gordon.** 2000. Localization of protease-activated receptors-1 and -2 in human mast cells: indications for an amplified mast cell degranulation cascade. Biotech. Histochem. **75:**85–90.
20. **Dileepan, K. N., and D. J. Stechschulte.** 2006. Endothelial cell activation by mast cell mediators. Methods Mol. Biol. **315:**275–294.
21. **Ferrell, W. R., J. C. Lockhart, E. B. Kelso, L. Dunning, R. Plevin, S. E. Meek, A. J. Smith, G. D. Hunter, J. S. McLean, F. McGarry, R. Ramage, L. Jiang, T. Kanke, and J. Kawagoe.** 2003. Essential role for proteinase-activated receptor-2 in arthritis. J. Clin. Invest. **111:**35–41.
22. **Gekara, N. O., and S. Weiss.** 2008. Mast cells initiate early anti-*Listeria* host defenses. Cell Microbiol. **10:**225–236.
23. **Genco, R. J.** 1992. Host responses in periodontal diseases: current concepts. J. Periodontol. **63:**338–355.
24. **Gunter, K. C., R. N. Germain, R. A. Kroczek, T. Saito, W. M. Yokoyama, C.**

Chan, A. Weiss, and E. M. Shevach. 1987. Thy-1-mediated T-cell activation requires coexpression of CD3/Ti complex. Nature **326:**505–507.

25. **Haeryfar, S. M., and D. W. Hoskin.** 2004. Thy-1: more than a mouse pan-T cell marker. J. Immunol. **173:**3581–3588.

26. **Harrington, L. E., P. R. Mangan, and C. T. Weaver.** 2006. Expanding the effector CD4 T-cell repertoire: the Th17 lineage. Curr. Opin. Immunol. **18:**349–356.

27. **Holt, S. C., J. Ebersole, J. Felton, M. Brunsvold, and K. S. Kornman.** 1988. Implantation of *Bacteroides gingivalis* in nonhuman primates initiates progression of periodontitis. Science **239:**55–57.

28. **Holzhausen, M., L. C. Spolidorio, R. P. Ellen, M. C. Jobin, M. Steinhoff, P. Andrade-Gordon, and N. Vergnolle.** 2006. Protease-activated receptor-2 activation: a major role in the pathogenesis of *Porphyromonas gingivalis* infection. Am. J. Pathol. **168:**1189–1199.

29. **Holzhausen, M., L. C. Spolidorio, and N. Vergnolle.** 2005. Proteinase-activated receptor-2 (PAR2) agonist causes periodontitis in rats. J. Dent. Res. **84:**154–159.

30. **Honda, T., Y. Aoki, N. Takahashi, T. Maekawa, T. Nakajima, H. Ito, K. Tabeta, T. Okui, K. Kajita, H. Domon, and K. Yamazaki.** 2008. Elevated expression of IL-17 and IL-12 genes in chronic inflammatory periodontal disease. Clin. Chim Acta **395:**137–141.

31. **Imamura, T.** 2003. The role of gingipains in the pathogenesis of periodontal disease. J. Periodontol. **74:**111–118.

32. **Jacob, C., P. C. Yang, D. Darmoul, S. Amadesi, T. Saito, G. S. Cottrell, A. M. Coelho, P. Singh, E. F. Grady, M. Perdue, and N. W. Bunnett.** 2005. Mast cell tryptase controls paracellular permeability of the intestine: role of protease-activated receptor 2 and beta-arrestins. J. Biol. Chem. **280:**31936–31948.

33. **Jawdat, D. M., G. Rowden, and J. S. Marshall.** 2006. Mast cells have a pivotal role in TNF-independent lymph node hypertrophy and the mobilization of Langerhans cells in response to bacterial peptidoglycan. J. Immunol. **177:**1755–1762.

34. **Kelso, E. B., J. C. Lockhart, T. Hembrough, L. Dunning, R. Plevin, M. D. Hollenberg, C. P. Sommerhoff, J. S. McLean, and W. R. Ferrell.** 2006. Therapeutic promise of proteinase-activated receptor-2 antagonism in joint inflammation. J. Pharmacol. Exp. Ther. **316:**1017–1024.

35. **Kramer, S., G. Sellge, A. Lorentz, D. Krueger, M. Schemann, K. Feilhauer, F. Gunzer, and S. C. Bischoff.** 2008. Selective activation of human intestinal mast cells by *Escherichia coli* hemolysin. J. Immunol. **181:**1438–1445.

36. **Leyton, L., A. F. Quest, and C. Bron.** 1999. Thy-1/CD3 coengagement promotes TCR signaling and enhances particularly tyrosine phosphorylation of the raft molecule LAT. Mol. Immunol. **36:**755–768.

37. **Li, T., and S. He.** 2006. Induction of IL-6 release from human T cells by PAR-1 and PAR-2 agonists. Immunol. Cell Biol. **84:**461–466.

38. **Lindner, J. R., M. L. Kahn, S. R. Coughlin, G. R. Sambrano, E. Schauble, D. Bernstein, D. Foy, A. Hafezi-Moghadam, and K. Ley.** 2000. Delayed onset of inflammation in protease-activated receptor-2-deficient mice. J. Immunol. **165:**6504–6510.

39. **Lourbakos, A., J. Potempa, J. Travis, M. R. D'Andrea, P. Andrade-Gordon, R. Santulli, E. J. Mackie, and R. N. Pike.** 2001. Arginine-specific protease from *Porphyromonas gingivalis* activates protease-activated receptors on human oral epithelial cells and induces interleukin-6 secretion. Infect. Immun. **69:**5121–5130.

40. **Lubberts, E., L. A. Joosten, M. Chabaud, L. van Den Bersselaar, B. Oppers, C. J. Coenen-De Roo, C. D. Richards, P. Miossec, and W. B. van Den Berg.** 2000. IL-4 gene therapy for collagen arthritis suppresses synovial IL-17 and osteoprotegerin ligand and prevents bone erosion. J. Clin. Invest. **105:**1697–1710.

41. **Lubberts, E., L. A. Joosten, F. A. van de Loo, P. Schwarzenberger, J. Kolls, and W. B. van den Berg.** 2002. Overexpression of IL-17 in the knee joint of collagen type II immunized mice promotes collagen arthritis and aggravates joint destruction. Inflamm. Res. **51:**102–104.

42. **Macfarlane, S. R., M. J. Seatter, T. Kanke, G. D. Hunter, and R. Plevin.** 2001. Proteinase-activated receptors. Pharmacol. Rev. **53:**245–282.

43. **Noorbakhsh, F., S. Tsutsui, N. Vergnolle, L. A. Boven, N. Shariat, M. Vodjgani, K. G. Warren, P. Andrade-Gordon, M. D. Hollenberg, and C. Power.** 2006. Proteinase-activated receptor 2 modulates neuroinflammation in experimental autoimmune encephalomyelitis and multiple sclerosis. J. Exp. Med. **203:**425–435.

44. **O'Brien-Simpson, N. M., R. A. Paolini, B. Hoffmann, N. Slakeski, S. G. Dashper, and E. C. Reynolds.** 2001. Role of RgpA, RgpB, and Kgp proteinases in virulence of *Porphyromonas gingivalis* W50 in a murine lesion model. Infect. Immun. **69:**7527–7534.

45. **O'Brien-Simpson, N. M., R. A. Paolini, and E. C. Reynolds.** 2000. RgpA-Kgp peptide-based immunogens provide protection against *Porphyromonas gingivalis* challenge in a murine lesion model. Infect. Immun. **68:**4055–4063.

46. **O'Brien-Simpson, N. M., P. D. Veith, S. G. Dashper, and E. C. Reynolds.** 2004. Antigens of bacteria associated with periodontitis. Periodontol. 2000 **35:**101–134.

47. **Oliver, R. C., and L. J. Brown.** 1993. Periodontal diseases and tooth loss. Periodontol. 2000 **2:**117–127.

48. **Ossovskaya, V. S., and N. W. Bunnett.** 2004. Protease-activated receptors: contribution to physiology and disease. Physiol. Rev. **84:**579–621.

49. **Pathirana, R. D., N. M. O'Brien-Simpson, G. C. Brammar, N. Slakeski, and E. C. Reynolds.** 2007. Kgp and RgpB, but not RgpA, are important for *Porphyromonas gingivalis* virulence in the murine periodontitis model. Infect. Immun. **75:**1436–1442.

50. **Potempa, J., R. Pike, and J. Travis.** 1997. Titration and mapping of the active site of cysteine proteinases from *Porphyromonas gingivalis* (gingipains) using peptidyl chloromethanes. Biol. Chem. **378:**223–230.

51. **Rege, T. A., and J. S. Hagood.** 2006. Thy-1 as a regulator of cell-cell and cell-matrix interactions in axon regeneration, apoptosis, adhesion, migration, cancer, and fibrosis. FASEB J. **20:**1045–1054.

52. **Schmidlin, F., S. Amadesi, K. Dabbagh, D. E. Lewis, P. Knott, N. W. Bunnett, P. R. Gater, P. Geppetti, C. Bertrand, and M. E. Stevens.** 2002. Protease-activated receptor 2 mediates eosinophil infiltration and hyperreactivity in allergic inflammation of the airway. J. Immunol. **169:**5315–5321.

53. **Shelburne, C. P., J. B. McLachlan, and S. N. Abraham.** 2006. *In vivo* models for studying mast cell-dependent responses to bacterial infection. Methods Mol. Biol. **315:**363–381.

54. **Steinsvoll, S., K. Helgeland, and K. Schenck.** 2004. Mast cells: a role in periodontal diseases? J. Clin. Periodontol. **31:**413–419.

55. **Stenton, G. R., O. Nohara, R. E. Dery, H. Vliagoftis, M. Gilchrist, A. Johri, J. L. Wallace, M. D. Hollenberg, R. Moqbel, and A. D. Befus.** 2002. Proteinase-activated receptor (PAR)-1 and -2 agonists induce mediator release from mast cells by pathways distinct from PAR-1 and PAR-2. J. Pharmacol. Exp. Ther. **302:**466–474.

56. **Tancharoen, S., K. P. Sarker, T. Imamura, K. K. Biswas, K. Matsushita, S. Tatsuyama, J. Travis, J. Potempa, M. Torii, and I. Maruyama.** 2005. Neuropeptide release from dental pulp cells by RgpB via proteinase-activated receptor-2 signaling. J. Immunol. **174:**5796–5804.

57. **Uehara, A., K. Muramoto, H. Takada, and S. Sugawara.** 2003. Neutrophil serine proteinases activate human non-epithelial cells to produce inflammatory cytokines through protease-activated receptor 2. J. Immunol. **170:**5690–5696.

58. **Uehara, A., S. Sugawara, K. Muramoto, and H. Takada.** 2002. Activation of human oral epithelial cells by neutrophil proteinase 3 through protease-activated receptor-2. J. Immunol. **169:**4594–4603.

59. **Vernal, R., N. Dutzan, A. Chaparro, J. Puente, M. Antonieta Valenzuela, and J. Gamonal.** 2005. Levels of interleukin-17 in gingival crevicular fluid and in supernatants of cellular cultures of gingival tissue from patients with chronic periodontitis. J. Clin. Periodontol. **32:**383–389.

Editor: A. J. Bäumler